DIAGNOSTYKA, 2024, Vol. 25, No. 1

e-ISSN 2449-5220
DOI: 10.29354/diag/176292

FAULT DETECTION AND DIAGNOSIS OF SQUIRREL CAGE ASYNCHRONOUS MOTOR USING A NEW COMSOL MULTIPHYSICS SOFTWARE 6.0

Benrabeh DJAIDIR [*], **Bachir NAIL**, **Abdelkader ROUIBAH**

Faculty of Science and Technology, University of Djelfa 17000 DZ, Algeria
[*] Corresponding author, e-mail: b.djaidir@univ-djelfa.dz

Abstract

In this paper, the diagnosis of faults in squirrel cage asynchronous motor and experimental analysis process are presented. Currently there are several simulation tools, that lets users analyze and interpret the behavior of their devices. Based on this, there is a lot of researches that is working on developing models, to detect and classify 3-phase asynchronous motor faults, significantly in the early stages. This work proposed design and experimental analysis established in Comsol Multiphysics 6.0 , which implements finite element analysis software (FEM) for detecting and diagnosing broken bar rotors of this types motors and its practical application. In this case, the post processor of the COMSOL-Multiphysics makes it possible to visualize in 2D the various magnetic and mechanical quantities. Through the curves of the magnetic flux density and analysis distribution of the field with magnetic induction lines, we can draw some conclusions, where we proposed an strategy, for detecting and diagnosing faults consistent with the structure of the software.

Keywords: Asynchronous Motor, Comsol Multiphysics, Diagnosis, Fault Detection, Flux Density.

1. INTRODUCTION

In the reality, electrical machines play an important role in modern industry and household applications, they are used to convert electrical energy into mechanical energy, and vice versa. Due to their robustness, simplicity of construction and low cost, with these characteristics they consume 35%–40% of the generated electric energy worldwide [1].

Asynchronous motors, is designated by the abbreviations ASM or IM, they represent now account for almost half of total electricity use in industrialized countries. This type of motors has state-of-the-art technology ensuring, high reliability, good starting torque and low maintenance cost [2, 3]. Electric motors of this series with a squirrel-cage rotor, which are controlled by a frequency converter with a supply voltage frequency of up to 400 Hz for example, have rotation speeds up to 30,000 rpm and higher [4].

Despite that the Squirrel cage 3-phase asynchronous motors is robust, it can sometimes present different types of defects, which can be either of electrical origin, or mechanical. Also, during the transient and steady-state, these motors produce a significant level of torque pulses, which create noise and vibration in the electric machine [5]. Monitoring and diagnosis require both a good functional and behavioral knowledge of the system in order to highlight in an early way the conditions leading to a failure situation. Thus, correct motor modelling is the first step in the detection of motor anomalies [6]. In this context, vibration analysis plays a vital role not only in diagnosing machinery condition for maintenance purposes, but also in the acceptance of new or recently overhauled equipment [7, 8].

On the other side, two types of defects may appear to the rotor in this type machine. The cage being composed of bars and short-circuit rings made of aluminum or copper, therefore a partial or total breakage of one of these components can be considered as electrical fault. The appearance of this type of defect can be due to several phenomena that are often independent of each other, such as improper use of the machine for example, an application of too much load or the environment in which the machine operates [9, 10].

A broken bar is one of the most frequent defects in the rotor. This defect can appear either at the notch or at the end which connects it to the rotor ring. The deterioration of the bars reduces the average value of the electromagnetic torque, increases the amplitude of the oscillations causing the rotation speed, which generates mechanical vibrations, therefore abnormal operation of the machine [11,12].

There are a variety of techniques for diagnosing and detecting defects, a lot of it based on observation and measurement, such as the measurement of the

Received 2023-08-18; Accepted 2023-12-04; Available online 2023-12-19

magnetic field, noise, vibration, current...Others depend on the monitoring and comparison of the electromechanical characteristics with those of the healthy motor (stator current, electromagnetic torque, and mechanical speed) [13]. In order to better situate our work, it was necessary to research what methods are used to diagnose and detect faults in the asynchronous machine.

In the field of electromagnetism, COMSOL Multi-Physics is a general simulation program for designing models, devices, and scientific research, the authors of Multisphysics uses finite elements and multiple physics simulations to solve problems and offers an identical user experience and interface regardless of the physical phenomena and the application studied. This program contains solutions for the following points: linear transformation coefficient analysis, limit analysis and timing-dependent problems [14, 15].

The user defines his couplings or selects the predefined interfaces. The different steps of the modeling process - defining the geometry, the material properties, the mesh, choosing the physics, solving and displaying the results - are integrated into a single interface[16, 17].

In this work we will explain the different steps to draw the geometry of the machine studied by Comsol Multiphysiques version 6.0, choose and introduce the physical properties of the different sub-domains (stator, rotor, air gap between rotor and stator), as well as the periodic boundary conditions, perform the mesh and then solve.

We applied tests on the operation of the studied machine with regard to the breakage of rotor bars because, broken rotor bar is one of the common machines malfunctions that may cause serious defects to the motor if it is not detected at a specific time. The magnetic flux leakage technique "MFL" tested with the software in order to simulate a rotor which contains defects, and to allow a better analysis of the responses with a new 2D model simulation.

2. MODELLING APPROACH

2.1 Maxwell’s equations in material media

Solving a problem in electromagnetism consists in determining the structures of the electromagnetic field in a region of space. These field configurations must simultaneously satisfy Maxwell's equations, and appropriate boundary conditions exact or analytical solutions can be obtained in a small number of cases depending on the geometry of the objects [18].

Maxwell's equations describe exactly how electric (E-fields) and magnetic fields (H-fields) behave, in the presence of matter. In this case standard notation are given by :

$$\nabla . E(r,t) = \frac{\rho_{total}(r,t)}{\varepsilon_0} \quad (1)$$

$$\nabla . B(r,t) = 0 \quad (2)$$

$$\nabla \times E(r,t) = -\frac{\partial B(r,t)}{\partial t} \quad (3)$$

$$\nabla \times B(r,t) = \mu_0 J_{total}(r,t) + \mu_0\, \varepsilon_0 \frac{\partial E(r,t)}{\partial t} \quad (4)$$

Where , and , are magnetic permeability of vacuum and the electric permittivity, respectively, and ; is the total charge density [19].

Discussion:

- It is a system of differential equations, which from a distribution of charges and current makes it possible to determine , , in all space at any time.
- Under real conditions (the distributions are of finite extension), we impose: , .
- If E is solution of Maxwell's equations, then , where is a uniform and stationary field is also a solution.
- We find the equations of electrostatics and magnetostatics.
- There are two large groups of Maxwell equations:
  - The divergence equations, which do not couple E and B.
  - The rotational equations, which couple E and B . Thus, in the general case, it is not possible to decoupling the two fields. (This is why, we are talking about an electromagnetic field).

Two related vector fields are used in physics to describe magnetic phenomena and can therefore the generic name of this definition is "magnetic field" [20], this concept which makes it possible to describe how the magnetic force is distributed in space around and inside a magnetic bodies, we take for example, the definitions of auxiliary fields as follows:

$$\mathrm{D}(r,t) = \varepsilon_0 \mathrm{E}(r,t) + \mathrm{P}(r,t) \quad (5)$$

$$\mathrm{H}(r,t) = \frac{1}{\mu_0}\mathrm{B}(r,t) - \mathrm{M}(r,t) \quad (6)$$

Where, is the magnetization field, and, is the polarization field, which are defined in terms of microscopic bound charges and bound currents respectively.

The macroscopic bound charge density, and bound current density, in terms of magnetization, and polarization; are then defined as:

$$\rho_b = -\nabla . \mathrm{P} \quad (7)$$

$$\mathrm{J_b} = \nabla \times \mathrm{M} + \frac{\partial B}{\partial t} \quad (8)$$

2.2 Finite element method (FEM)

This method is based on the numerical resolution of Maxwell's equations, the information provided by this type of simulation is very precise and allows us to take into account the geometry of the machine, the saturation effect of magnetic materials, as well as the effects of harmonics in space.

Maxwell's equations arise in two dual systems:

- The laws of Faraday and flux conservation (magnetic system)

- The Ampère-Maxwell and Gauss theorems (electrical system).

Summing it up, the example of diagrammatic presentations of physical theories is the so-called Maxwell's house, which present Maxwell's equations for electric and magnetic fields. The duality of the two systems can be highlighted using the Tonti diagram [21]. As a result, it is possible to represent all these data geometrically, using the Tonti diagram which is applied to electromagnetism as shown in figure 1.

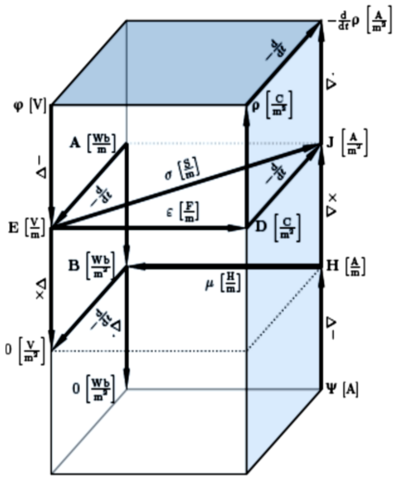

Fig. 1. Maxwell's house or Tonti's diagram for continuous electromagnetic quantities

To illustrate, the Tonti diagram is composed of Maxwell's equations, the laws of behavior, electrical and magnetic quantities, potentials and their spaces . Through the Gauss's law for magnetism by the equation (2), we know that B is a solenoid vector field and therefore, using Helmholtz decomposition, the magnetic field can be explained as the curl of some other vector field which will be the magnetic vector potential A, with , [22]:

$$\mathrm{B} = \nabla \times \mathrm{A}, \qquad (9)$$

Substituting equation (9), in Maxwell-Faraday's law:

$$\nabla \times \mathrm{E} = -\frac{\partial}{\partial \mathrm{t}}\mathrm{B} = -\frac{\partial}{\partial \mathrm{t}}\nabla \times \mathrm{A} = -\nabla \times \frac{\partial}{\partial \mathrm{t}}\mathrm{A}, \quad \rightarrow$$

$$\nabla \times \left(\mathrm{E} + \frac{\partial}{\partial \mathrm{t}}\mathrm{A}\right) = 0 \qquad (10)$$

Thus, we can express this quantity using the gradient of another scalar field, the so-called electric scalar potential, as follow:

$$\mathrm{E} = -\nabla\varphi - \frac{\partial}{\partial \mathrm{t}}\mathrm{A} \qquad (11)$$

In summary, diagrams and their morphisms give us a solid theoretical framework with which to describe systems of equations and their solutions.

The equations that describe the electromagnetic coupling between magnetic effects and electrical effects can be decoupled in some cases, giving rise to simpler models. Therefore, the model equations become [23]:

$$\circ \quad \begin{cases} \vec{D} = \varepsilon\vec{E} \\ \vec{B} = \mu\vec{H} + \vec{B}_r \\ \vec{J} = \sigma\left(\vec{E} + \vec{v}\wedge\vec{B}\right) \end{cases} \qquad (12)$$

- Vector, represents the speed of displacement of the charges in the field B;
- Vector, represent the remanent induction.
- Coefficient, is the electrical permittivity, it is valid , in the case of vacuum and is superior for all other materials.
- Coefficient, is the electrical conductivity. It is zero in the vacuum case.
- Coefficient, is the magnetic permeability, it is equal to, in the case of vacuum is greater for all other magnetic materials.

To these equations must be associated the generalized Ohm law :

$$\vec{J} = \vec{J}_{ext} + \sigma\vec{E} + \sigma(\vec{\mu}\wedge\vec{B}) \qquad (13)$$

With , Excitation current density (source) [A/m^2]. , Density of the induced currents of the electric field [A/m^2]. And ; Density of motion-induced currents [A/m^2].

3. EXPERIMENTAL TESTS

Firstly, we conducts numerical simulation for experimental confirmation of theoretical studies, where the application consists of squirrel cage 3-phase asynchronous motor, with 4 pole (P), and 36 slots in the stator and 26 aluminum bars in the rotor for a supply frequency f = 50 Hz. Main important parameters of the motor are shown in table 1.

Figure 2, shows rotor slot type (unit: mm), the modeling and simulation was created in the finite element program, to finely represent the different sizes in the design, as an example.

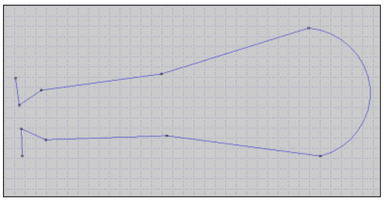

Fig. 2. Rotor slot type

The pre-processor of this technique (FEM), makes it possible to draw the different parts of the element to be studied, to define the materials used, also, for impose the boundary conditions and so on.

The design of motor model has been simulation by COMSOL multiphysics, for analyze the rotor part and plotted at various degrees. In this case, we chose the design on the basis of the typical values in the database of motor, when the operating conditions are moderate and certain conditions are met. Figure 3, show the model of the motor studied.

Table 1. Parameters of motor model

Name	Value	Description
I_0	3.677 A	Current amplitude
N	60	Number of turns
L	0.30 m	Length of motor
F_0	50 Hz	Supply frequency
W_0	314.16 Hz	Supply angular frequency
Air Gap	0.0020 m	Size of air gap
Z_1	36	Stator slots
Z_2	26	Rotor slots
η	80%	Efficiency

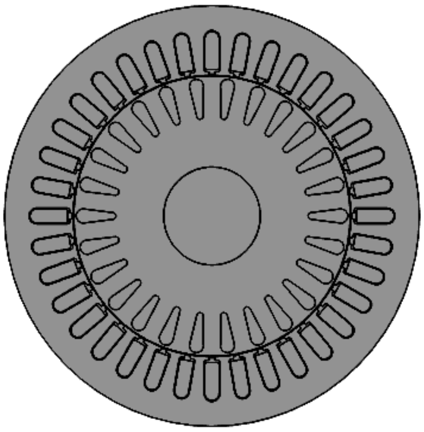

Fig. 3. Geometry of asynchronous machine

After selecting the model, the mesh is designed of our machine before the problem. The boundary conditions and the parameters of the model are specified. From figure 4, it can be clearly visible that when motor is under steady state situation, with Z_2 equal 32. In this case, we have adopted a mesh with triangular elements, as well as MFD magnetic flux density .

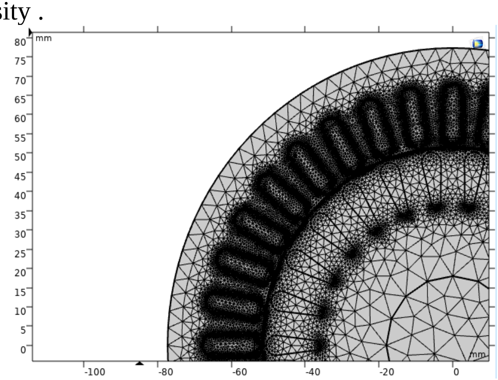

Fig. 4. Rotor and stator MFD distribution

In this part we are interested in the simulations of the machine in dynamic mode. We will determine the distribution of the magnetic potential vector and the distribution of the magnetic induction for given instants.

The field of study must be discretized (mesh) with geometrical elements which form a mesh where the physical sizes will be determined in any node. On the other hand, the geometric characteristics of the mesh can play a preponderant role when diffusive fluxes come into play.

The figure 5, shows the distribution of magnetic field lines through the contour, as well as the distribution of magnetic induction on the surface. Note that the maximum magnetic induction is 1.23 T.

It is noted that the distribution of the magnetic field lines is symmetrical and high in the vicinity of the stator notches because of the current flowing in the coils, thus these lines are less intense between the rotor bars and very low in the air. As well, it observed the regularity flux density on the distribution in general, and more uniform in density on the rotor part, figure 6.

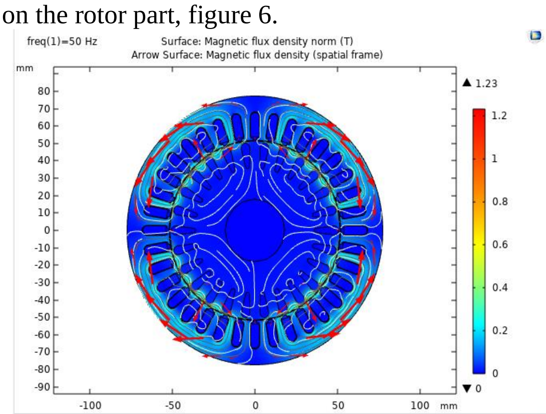

Fig. 5. Simulation of the squirrel cage ASM, with f=50 HZ

We simulated the ASM in 2 dimensions (2D), to visualize the distribution of magnetic field lines and magnetic induction in order to identify the parameters that define the domain of study.

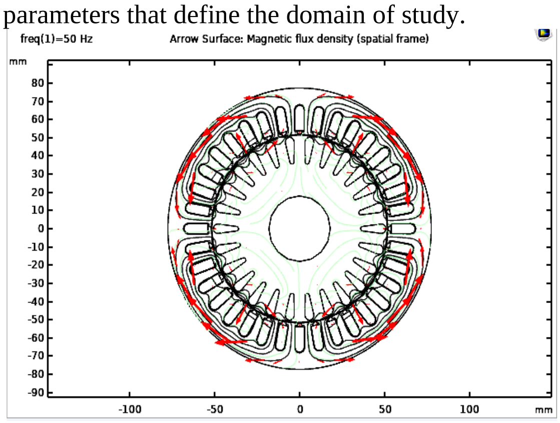

Fig. 6. Representation the direction of the magnetic field

The figure 7, represent the graph of magnetic flux density, in (x-component and y-component), as a result of total electromagnetic induction in healthy operations for the motor, this graph help us to obtain and explain the figure 08 .

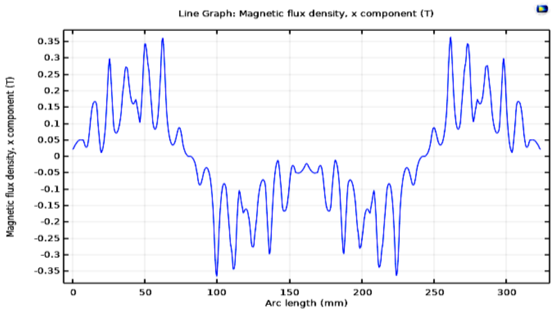

a)

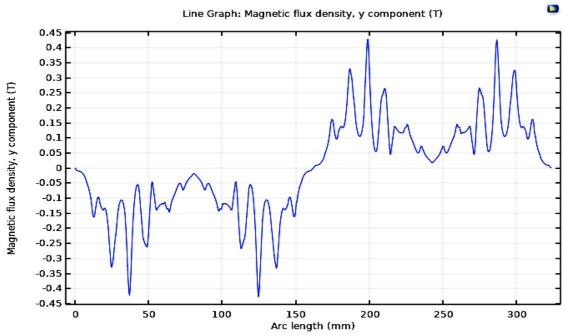

b)

Fig. 7. Magnetic flux density graph
a) The x-component ; b) The y-component

As can be seen from figure 8, for the healthy motor, the magnetic field lines remained symmetrical , when the poles and slots are symmetrically designed. The simulation results and the modeling of magnetodynamic phenomena of a 3-phase squirrel cage in a healthy state has been presented.

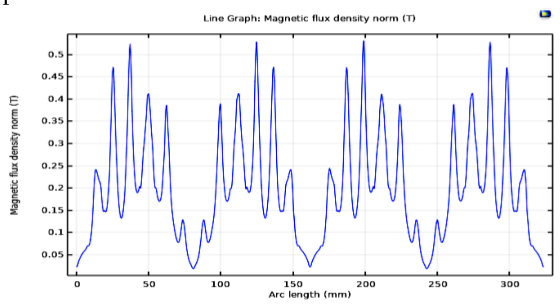

Fig. 8. Line graph of magnetic flux density norm in B , 4 pole

Meanwhile, digital simulation by COMSOL Multiphysics, offers a better understanding of physical phenomena. This software was used since it is a powerful calculation tool allowing to take into account the nonlinearities of the process and the interaction between phenomena of different nature.

This software contains three parts. Pre-processor, processor (solution), and post-processing.

- Create a finite element model(FEM), and prepare load parameters that belong to the pre-process;
- Mesh division and solving equations are all belong to solution part;
- Visualize and analyze results are belong to post- processing [13].

Figure 9, shows the diagram and design of geophysical forward modeling, using the studied software.

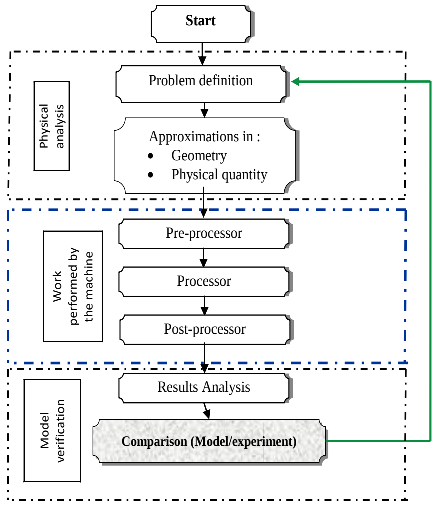

Fig. 9. Modeling steps by COMSOL MULTIPHYSICS

3.1. Application (01)

After having implemented the model described previously. In this part, we present the detection and characterization of broken rotor bars (BRBs), and analysis of magnetic field of dispersion. Reducing the value of the electrical conductivity of a rotor bar, for a first test, the value of 0 [S/m] will be taken, as illustrated in figure 10.

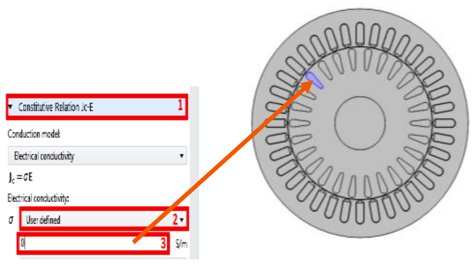

Fig. 10. Rotor bar fault

The electrical resistance of these bars is sufficiently low so that the currents it does not pass properly in the sheets. The short-circuit rings allow the circulation of currents from one rotor bar to the other, as a result the electromagnetic torque and mechanical speed fluctuations tend to increase with the number of faulty bars.

The results showed, that the dispersion of magnetic flux can give information about the presence of a defect as shows in figure 11, in this direction, rotor failure are caused by a group of different pressures that work on the rotor due to magnetic stresses , electromagnetic force wave imbalance, vibrations, and bearing defects, (BRBs) also cause an unbalanced current distribution between the rotor bars. The figure 12, shows the distribution of MFD in the 3-ph asynchronous motor, we presented their evolutions for the test with broken bar with zoom on the parts where is the defect.

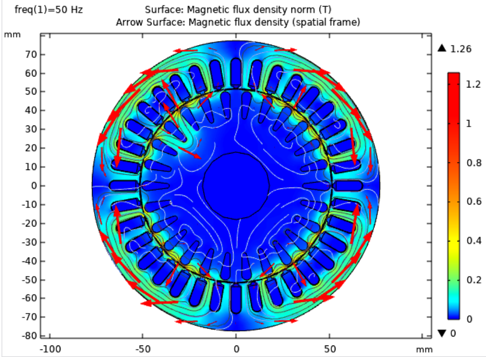

Fig. 11. Distribution of magnetic flux density, BRB

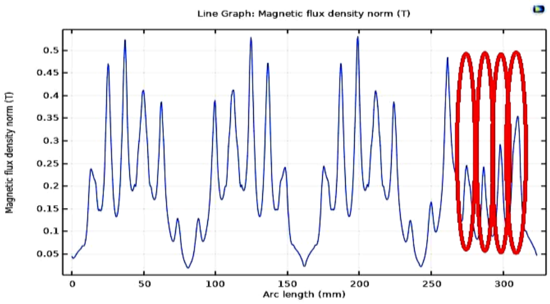

Fig. 12. Line graph of magnetic flux density BRB

More analytically, in the first application at the level of the software structure, we have established procedures for determining the inductors of an ASM with BRB fault under different load conditions according to the parameters of the model in the same ASM when it is healthy.

In the experimental results presented, we notice the lines of the field become more disturbed and they cluster around the broken bars. In this case, the current of the broken bar is practically zero. The currents at the level of the bars adjacent to the broken bar have assumed large values compared to the currents of the bars in the healthy state.

The deterioration of the bars reduces the average value of the electromagnetic torque and increases the amplitude of the oscillations, which themselves cause oscillations in the speed of rotation, which generates mechanical vibrations and therefore abnormal operation of the machine.

With this in mind, the presence of any fault causes an electrical and magnetic imbalance in the rotor, which affects the distribution of the magnetic field in the machine.

A reliable diagnosis therefore requires a good knowledge of the mechanisms of the faults to be monitored, as well as their consequences on the signals from the machine.

3.2. Application (02)

In the structure of the monitoring system that we propose, we are particularly interested in the stationary operating conditions, and for the abnormal operating modes.

The stresses that can help the appearance of a problem broken rotor bar are of origin:

- Mechanical, due to fatigue at the parts of the rotor and bearing defects.
- Electromagnetic.
- Thermals.
- Dynamic generated by shaft torques and/or centrifugal forces.
- Environmental, caused by humidity and dust.

The breaking of 4 bars in COMSOL-Multiphysics software, as illustrated in figure.13.

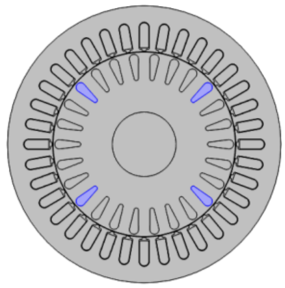

Fig. 13. Rotor bar fault BRB_s

In the same way, by simulation the figure 14, shows the distribution of the magnetic field lines, as well as the distribution of the magnetic induction with another form, the maximum induction is 1.33 T. Also, we observed the of non-uniform density flux, on the rotor distribution, and the density is dispersed and inconsistent. Figure 15, shows the line graph of MFD, with the breaking of 4 bars , detecting a fault is generally accomplished by monitoring the magnitude of specific components in the actual state of the controlled system taking into account these different modes of operation and making any necessary inferences to produce used data.

The use of this data then makes it possible to draw up operating histories, if necessary, to implement a failure treatment process.

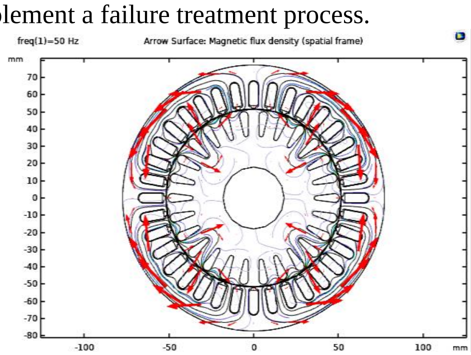

Fig. 14. Distribution of magnetic flux density, BRB_s

A broken bar fault does not cause the motor to stop, because the current which passed through the broken bar is distributed over the adjacent bars. At the same time if an appropriate diagnostic procedure is not taken these bars are then overloaded as a result, which can lead to their break and so on until the breaking or rupture of a sufficiently large number of bars to cause the motor to stop.

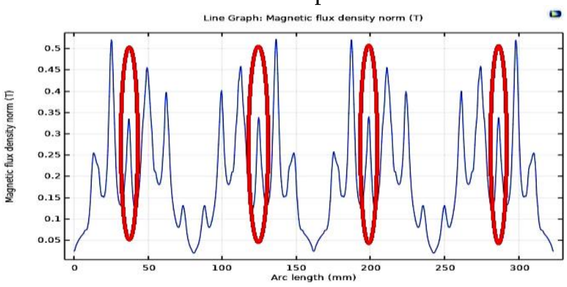

Fig. 15. Line graph of magnetic flux density, BRB_s

The results of magnetic simulations have been widely presented. These results are obtained from the COMSOL-Multiphysics software. Broken bars are the most common rotor faults, their simulations make it possible to identify the signatures of these faults and to predict the deteriorations generated in the machine.

In addition, one of the most important objectives, within the framework of the diagnosis, concerns the development of the most reliable simulation models possible, representing the faulty operation of the machine.

In summary, in this study we extended the approach to take into account the interaction of the electromagnetic problem with the magneto-mechanical effects at the rotor level in the motor, taking into account various phenomena such as local saturation, rotor inductance, and vibrations likely to affect the installation considered. Using the COMSOL multiphysics program, we analyzed the behavior of ASM in the healthy and faulty cases with different levels of indicators from measurements and permanently established. We were able to highlight the following points:

- The interest of the current approach proposed for determining the parameters of the asynchronous motor model is intrinsic, because it does not require heavy and long calculations for each configuration comparing with the other approaches.
- We have opted for the use of a software well dedicated to this type of machines, in light of its good use the internal models, based on the resolution analytical or numerical, of the fundamental equations of electromagnetism.
- The different results obtained by the COMSOL-Multiphysics software, which is based on the finite element method for all the cases of the asynchronous machine studied. This program facilitates us to model and simulate the electromagnetic and mechanical phenomena of this type of machine, simulation aimed at the general behavior of the machine in dynamic and permanent conditions, but which can be used more particularly in the field of fault diagnosis.

4. CONCLUSION

This work proposed design and experimental analysis in 3-phase asynchronous motor with COMSOL Multiphysics. This type of engine has state-of-the-art technology ensuring, versatility, foolproof reliability, energy-efficient, and a particularly long service life. Even so, the broken rotor bar fault are among the most common anomalies that affect this type of motors.

In this paper, a new study is proposed for the ASM, with the detection of BRBs, this technique based on use the flux density results and signal processing methods on COMSOL Multiphysics version 6.0, software allowing the strong coupling of several multi-physics models.

Therefore, the current approach proposed the monitoring and fault detection of the asynchronous motor by this program, is divided into two parts . The first part, is to apply the finite element method (FEM), which is in its role the calculation basis of the COMSOL software, furthemore, we have modeled and coupling phenomena of electromagnetic , with the magneto-mechanical effects in the program level, to develop an approximation of the magnetic field and their behavior, as well as magnetic flux density . Also a series of simulations was carried out, to validate the model in different situations for analyzing the steady state of a healthy motor.

The second part is to compare the simulation results with broke rotor bars, taking into account the relationship between the rotor path currents and the magnetic path flux and their distribution, as the matter of fact, this technique represent the behavior of magnetic field quantities in a way that allows us to more easily detect and diagnose these faults. A good detection procedure should take the minimum necessary steps from the process in question, as well as extract a diagnosis giving a clear indication of failure modes, through data analysis in a minimum of time.

We have done tests in the laboratory, the results found are satisfactory and are consistent in order to establish a general strategy for fault diagnosis in electrical machines in the future.

Funding: *The manuscript does not have external funds.*

Author contributions: ***r****esearch concept and design, B.D.; Collection and/or assembly of data, B.D.; Data analysis and interpretation, B.D., B.N.; Writing the article, B.D., B.N.; Critical revision of the article, B.D., B.N., A.R.; Final approval of the article, B.D.*

Declaration of competing interest: *The authors declare that they have no known competing financial interests or personal relationships that could have appeared to influence the work reported in this paper.*

REFERENCES

1. Zhao A, Zanuso G, Peretti L. Transient thermal models of induction machines under Interturn short-circuit fault conditions. IET Electric Power Applications, the institution of engineering and technology 2023; 1–17. https://doi.org/10.1049/elp2.12343.
2. Ahmed FS, Hussain ZS, Salih TKM. Enhancing performance for three-phase induction motor by changing the magnetic flux density and core material using COMSOL. International Journal of Electrical and Computer Engineering 2022; 12(1): 62-72. http//doi: 10.11591/ijece.v12i1.pp62-72.
3. Abdelhak G, Sid Ahmed B, Rabah D. Fault diagnosis of induction motors rotor using current signature with different signal processing techniques. Diagnostyka 2022; 23(2):1-9. https://doi.org/10.29354/diag/147462.
4. Ibragimov M, Akbarov D, Fayziyev M, Beytullaeva R, Nimatov K ,Safarov KhS. Analysis of the methods of diagnosing asynchronous motors according to vibration indicators. IOP Conf. Series: Earth and Environmental Science 2023. https://doi:10.1088/17551315/1142/1/012031.
5. Shadfar H, Izadfar HR. A New Squirrel Cage Rotor Structure to Improve the Dynamic Performance of the Single-Phase Induction Motor. International Journal of Industrial Electronics, Control and Optimization 2022; 5(4): 1-8. https://doi.org/10.22111/ieco.2022.42485.1431.
6. Venugopal G, Udayakumar AK , Balashanmugham A, Houran MA, Alsaif F, Elavarasan RM, Raju K, H. Alsharif M. Fault identification and classification of asynchronous motor drive using optimization approach with improved reliability. Energies 2023; 16(2660): 1-25. https://doi.org/10.3390/en16062660.
7. Djaidir B, Hafaifa A, Kouzou A. Faults detection in gas turbine rotor using vibration analysis under varying conditions. Journal of theoretical and applied mechanics 2017; 55(2): 393-406. https://doi.org/10.15632/jtam-pl.55.2.393.
8. Gubarevych O, Gerlici J, Gorobchenko O, Kravchenko K, Zaika D. Analysis of the features of application of vibration diagnostic methods of induction motors of transportation infrastructure using mathematical modelling. Diagnostyka 2023; 24(1): 1-10. https://doi.org/10.29354/diag/161308.
9. Cao Y, Liu X. Dynamic analysis of a mechatronic drive system with an induction motor. Journal of theoretical and applied mechanics 2023; 61(2): 245-258. https://doi.org/10.15632/jtam-pl/160178.
10. Amar R, Boubakeur Z, Djelali M, Larbi B. Detection of faults in the asynchronous machine by the use of smart materials. Diagnostyka 2018; 19(3): 43-54. https://doi.org/10.29354/diag/93230.
11. Hassan OE, Amer M, Abdelsalam AK, Williams BW. Induction motor broken rotor bar fault detection techniques based on fault signature analysis. The Institution of Engineering and Technology 2018; 12 (7): 895-907. https://doi.org/10.1049/iet-epa.2018.0054
12. Puche-Panadero R, Sarkimaki V, Rodriguez P. Detection of broken rotor bar fault in induction machine fed by frequency converter. Int. Symp. On Power Electronics. Electrical Drives 2012; 1027–1032. https://doi.org/10.1109/SPEEDAM.2012.6264470.
13. Mechefske Li W, Chris K M. Detection of induction motor faults: A comparison of stator current, vibration and acoustic methods. J. Vib. Control, 2006; 165–188. https://doi.org/10.1177/1077546306062097.
14. Wang, XH. Yue, Liu G, Zhao Z. The Application of COMSOL Multiphysics in Direct Current Method Forward Modeling. Xi'an International Conference on fine geological exploration and groundwater & gas hazards control in coal mines, Procedia Earth and Planetary Science 2011; 266–272. https://doi.org/10.1016/j.proeps.2011.09.093.
15. Kocman S, Pecinka P, Hruby T. Induction motor modeling using COMSOL multiphysics. 2016 17th International Scientific Conference on Electric Power Engineering (EPE). https://doi.org/10.1109/EPE.2016.7521727.
16. Bouneb I, Kerrour F. Nanometric modelization of gas structure, multidimensional using COMSOL software. International Journal of Electrical and Computer Engineering 2018; 8(4): 2014-2020. https://doi.org/10.11591/ijece.v8i4.pp2014-2020.
17. Faeq DT, Raafat J, Ali M. Comparison of magnetic flux density for six-phase and three-phase induction motor using COMSOL Multiphysics. Journal of Zankoy Sulaimani 2019; 1-10. https://doi: 10.17656/jzs.10752.
18. Chou W, Liang Y , Gao L, Wang D. Research on eddy current losses algorithm in solid rotor of high speed squirrel cage induction motor. Journal the institution of engineering and technology 2020; 14(6): 1023. https://doi.org/10.1049/iet-epa.2019.0884.
19. Hang S, Xue-Tao W. Application of COMSOL Multiphysics in thermal effect analysis of electromagnetic active vibration absorber. IOP Conf. Series: Materials Science and Engineering 2017; 269: 22-24. https://doi.org/10.1088/1757-899X/269/1/012037.
20. Xudong W. Aluminum loss analysis and evaluation of squirrel induction motor. Journal of computers 2013; 8(3): 749-755. https://doi.org/10.4304/jcp.8.3.749-755.
21. Piergiorgio A, Fabio F, Maurizio R. Multiphysics problems via the cell method. The Role of Tonti Diagrams. IEEE transactions on magnetic 2010; 46(8): 2959 – 2962. https://doi.org/10.1109/TMAG.2010.2044487
22. Piergiorgio A, Fabio F, Maurizio R, Carlo R. The Cell Method for Electrical Engineering and Multiphysics Problems . Lecture Notes in Electrical Engineering; 230. https://doi.org/10.1007/978-3-642-36101-2_1.
23. Vijaya S, Mohammadian HA, Hall WF. A Time-Domain, Finite-Volume Treatment for the Maxwell Equations. 2007; 127-145. https://doi.org/10.1080/02726349008908232.

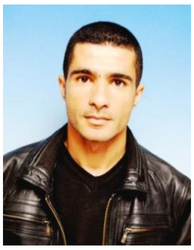

Benrabeh DJAIDIR: PhD degree in Electronic field, specializing in Automation in 2016 from University of Djelfa, Algeria. He is currently an Associate Professor in Control Engineering and Automation Systems in the Electrical Engineering Department at Ziane Achour University of Djelfa.
His research area of interests includes the Modelling and Control in Industrial Systems, the Diagnosis and new Reliability Engineering, Electrical and Mechanical system

modelling and Electromechanical System Fault Detection and Diagnosis.
Email: b.djaidir@univ-djelfa.dz

Bachir NAIL : PhD and HDR degree in Automatic Control field, Industrial Diagnosis specialty. Professor (Associate) at Ziane Achour University of Djelfa.
My research interests include, but not limited to the following areas: Fault Tolerant Control (FTC) and Fault Detection (FD) , for Multivariable Systems, Matrix Polynomial Theory, Estimation/Identification of Dynamical Systems.
e-mail: b.nail@univ-djelfa.dz

Abdelkader ROUIBAH: He received the state engineer degree in Mechanical engineering specialized energy from the University of Msila (Algeria) in 1992, and the Master's degree in Industrial Maintenance from Boumerdes University (Algeria) in 2012, and PhD in Mechanical Engineering "Option: Renewable Energy" at the same university in 2020. He is currently working as a lecturer at the University of Djelfa since 2013. His research interests are solar thermodynamics (power plants from solar towers).
e-mail: a.rouibah@univ-djelfa.dz